Antifouling Polymer Membranes with Subnanometer Size Selectivity

Ariya Akthakul,[†] Richard F. Salinaro,[‡] and Anne M. Mayes*[,†]

Department of Materials Science & Engineering, Massachusetts Institute of Technology, Cambridge, Massachusetts 02139, and Pall Corporation, Port Washington, New York 11050

Received June 12, 2004; Revised Manuscript Received July 28, 2004

ABSTRACT: Membranes that deliver nanoscale size selectivity are desirable for applications ranging from water treatment to molecular separations. Here we describe polymer thin film composite membranes coated with amphiphilic graft copolymers consisting of a poly(vinylidene fluoride) (PVDF) backbone and poly(oxyethylene methacrylate) (POEM) side chains, PVDF-*g*-POEM. Transmission electron microscopy and thermal analysis reveal that these materials molecularly self-assemble into bicontinuous nanophase domains of semicrystalline PVDF, providing structural integrity, and poly(ethylene oxide) (PEO), providing selective transport channels of defined size. PVDF ultrafiltration membranes coated with PVDF-*g*-POEM wet instantaneously and reject >99.9% of emulsified oil from a 1000 ppm oleic acid/triethanolamine/water microemulsion feed at 66 psi without fouling. Their molecular sieving capability is demonstrated through separation of like-charged organic dyes varying in molecular dimensions by several angstroms. Thicker films of PVDF-*g*-POEM also act as a chromatograph, exhibiting time-dependent permeation of vitamins B_2 and B_{12}. Nonporous asymmetric membranes prepared by immersion precipitation of PVDF/PVDF-*g*-POEM blend solutions exhibit separation capability similar to that of the thin film composites. These new nanochannel membranes hold potential utility for both high volume and high end value liquid-based separations.

I. Introduction

With the continuing decline of available freshwater supplies, recycling of municipal, industrial, and commercial wastewater has gained the spotlight in recent environmental policy.[1] The cleaning of oily water wastes has been a challenging aspect of water treatment, particularly the removal of oily microemulsions, where stabilized droplet sizes as small as 10 nm are known to occur.[2] Nanofiltration (NF) membranes are effective in the removal of such species but often suffer from low flux due to limited permeability and surface fouling.[3,4]

Membrane technologies with subnanometer fractionation capability hold further promise for high end value molecular separations in the chemical, biochemical, and pharmaceutical industries.[5−8] Molecular sieving membranes offer potential advantages of scalability, speed, and cost efficiency compared with competing technologies such as chromatography and electrophoresis.[9] To date, however, few examples of such membranes have been reported.[10−13] For instance, Martin and co-workers prepared gold nanotubule membranes by electroless Au deposition into the cylindrical pores of a commercial track-etched polycarbonate membrane and demonstrated size-based separation of molecule mixtures such as pyridine (79 Da) and quinine (324 Da).[10] By chemisorbing thiol-terminated poly(ethylene glycol) to the Au nanopore surfaces, this group further achieved size-based separation of globular proteins while avoiding internal fouling.[11] As an alternate approach, Snurr and co-workers fabricated membranes from thin films of "molecular squares" having cavities of 18−20 Å coated on a porous polyester support membrane and demonstrated the separation of Fe(1,10-phenanthroline)$_3^{2+}$ ($d \sim 13$ Å) from Fe(4,7-phenylsulfonate-1,10-phenanthroline)$_3^{4-}$ ($d \sim 24$ Å).[12]

Achieving molecular-level size selectivity with conventional polymer membranes remains a major challenge because the immersion precipitation process widely used to make porous commercial membranes today typically results in a separation layer exhibiting sparse porosity and broad pore size distribution.[14] The process of direct beam etching allows for fabrication of nucleopore membranes[15] with nanometer-scale pores of uniform size, such as those used by Martin;[10,11] however, this method is expensive and yields low porosity (∼2−3%).[16] Hence, the ability to create uniform molecular sieving channels of high density in polymer membranes made by immersion precipitation could widely impact the cost and efficiency of liquid-based nanoscale separations.

To address this need, this work describes a new class of nanochannel membranes made from a commercial poly(vinylidene fluoride) (PVDF) ultrafiltration membrane coated with a micron-scale film of an amphiphilic graft copolymer consisting of a PVDF backbone and side chains of poly(oxyethylene methacrylate) (POEM).[17] The PVDF-*g*-POEM coating molecularly self-assembles into continuous nanophase domains of semicrystalline PVDF interweaved with nanochannels of poly(ethylene oxide), providing a mechanism for size-selective transport. The PEO component serves a secondary role as a steric/enthalpic barrier to surface fouling by oils and biological molecules.[18] We show herein that such membranes give dramatic flux enhancement in oily water filtration over a commercially available NF membrane and demonstrate further promise for rapid, molecular-scale separations.

II. Experimental Section

Materials. Poly(vinylidene fluoride) (PVDF, $M_n \sim 107\,000$ g/mol), copper(I) chloride (CuCl), 4,4′-dimethyl-2,2′-dipyridyl (DMDP), 1-methyl-2-pyrrolidinone (NMP), dimethylformamide (DMF), dimethylacetamide (DMAc), oleic acid, triethanolamine, alcian blue (pyridine variant), rhodamine B, brilliant

[†] Massachusetts Institute of Technology.
[‡] Pall Corporation.
* Corresponding author: e-mail amayes@mit.edu.

10.1021/ma048837s CCC: $27.50
Published on Web 09/03/2004

blue, congo red, vitamin B_2, vitamin B_{12}, and poly(ethylene glycol) methyl ether methacrylate, referred to herein as poly(oxyethylene methacrylate) $POEM_9$ ($M_n \sim 475$ g/mol) and $POEM_{23}$ ($M_n \sim 1100$ g/mol), were purchased from Sigma-Aldrich (Milwaukee, WI) and used as received. Petroleum ether, ethanol, and deuterated DMF were obtained from VWR. All solvents were reagent grade and used as received. Deionized water (dW) of 18 MΩ·cm resistivity was prepared using a Millipore (Bedford, MA) Milli-Q filtration system.

Graft Copolymer Synthesis. Atom transfer radical polymerization (ATRP) allows for the preparation of graft copolymers from polymer macroinitiators incorporating pendant chemical groups containing radically transferable halogen atoms.[19,20] PVDF-*g*-POEM copolymers were synthesized by atom transfer radical polymerization using PVDF (Sigma-Aldrich, 107 kg/mol, $M_w/M_n = 2.4$) as a macroinitiator, following methods outlined previously.[17,21] The reaction times were varied according to the size-dependent reactivity of POEM macromonomers, proceeding for 19 h for PVDF-*g*-$POEM_9$ and 36 h for PVDF-*g*-$POEM_{23}$.

Characterization of Graft Copolymers. POEM content of the PVDF-*g*-POEM copolymers was determined by ^1H nuclear magnetic resonance (NMR) in deuterated DMF using a Bruker DPX 400 spectrometer. The number-average molecular weight of each copolymer was subsequently calculated on the basis of the concentration of POEM present and the number-average molecular weight of the parent PVDF reported by the manufacturer.

Crystallinity of PVDF and POEM in the PVDF-*g*-POEM copolymers was investigated by differential scanning calorimetry (DSC) using a TA Instruments Q1000 calorimeter and by X-ray diffractometry (XRD) using a Rigaku Rotaflex RTP500 RC. Prior to each measurement, the copolymers were dried in air for over 12 h and subsequently placed under vacuum overnight at room temperature. For DSC measurements, samples were precooled to −100 °C and then heated and cooled at 20 °C/min between −100 and 200 °C prior to the measurement. DSC thermograms were recorded from the subsequent reheating at 20 °C/min from −100 to 200 °C. The weight percent PVDF crystallinity in PVDF-*g*-POEM samples was calculated from the ratio of the heat of melting from the DSC thermograms and the reported heat of fusion of PVDF (101.5 J/g),[22] normalized by the weight fraction of PVDF in each copolymer determined from NMR. X-ray diffraction patterns were collected in the angular range $2\theta = 5°-60°$ at the rate of 1°/min using a monochromatic Cu Kα source ($\lambda = 0.154$ nm).

Transmission electron microscopy (TEM) studies of the graft copolymer morphology were performed on cryomicrotomed sections of PVDF-*g*-POEM on a JEOL 200CX microscope operated in bright field mode at 100 kV, as described in a previous publication.[17] POEM domains were stained with RuO_4 to enhance contrast.

Membrane Preparation. Free-standing films ∼500 μm in thickness were obtained by evaporation casting 20 mL of a 20 wt % solution of graft copolymer in DMF onto a flat Teflon dish 10 cm in diameter. The solvent was subsequently allowed to evaporate slowly on a hot plate at 60 °C over 24 h under the hood. Composite membranes were prepared by coating a ∼3.5 μm thick PVDF-*g*-$POEM_9$ layer onto porous PVDF ultrafiltration membranes (Pall Corp. DV-20) using a proprietary coating technique (Pall Corp.). Nonporous asymmetric membranes with a PVDF-*g*-POEM rich separating layer were fabricated by immersion precipitation.[17] A 200 g/L polymer solution containing a 25 wt % blend of PVDF-*g*-$POEM_9$ in PVDF dissolved in DMAc served as the casting solution.

Membrane surface and cross-sectional morphology were investigated using a JEOL 6320 field emission scanning electron microscope (FESEM) operating at 1 kV.[17] Freeze-fractured membrane samples were sputter-coated with gold−palladium for SEM imaging. The wetting behavior of composite membranes and PVDF film controls was investigated using a VCA2000 video contact angle system from Advanced Surface Technologies.

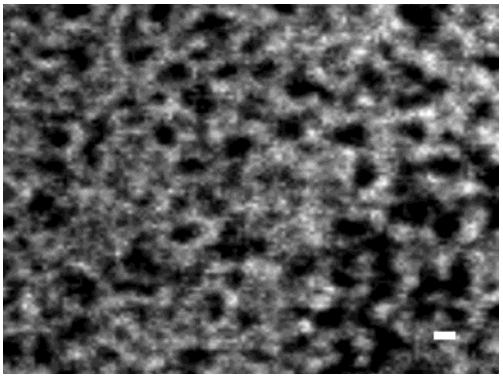

Figure 1. TEM image of PVDF-*g*-$POEM_9$ nanodomain morphology, showing interconnected PVDF domains (bright phase). Scale bar is 2 nm.

Filtration Experiments. Filtration experiments on solvent cast thick films were performed on 49 mm diameter membranes using a SEPA stirred, dead-end filtration cell (Osmonics) having an effective filtration area of 16.9 cm^2. Filtration experiments with thin film composite membranes were performed on 43 mm diameter membranes using an Amicon 8050 stirred, dead-end filtration cell (Millipore) having an effective filtration area of 13.4 cm^2 and on 25 mm diameter membranes using an Amicon 8010 stirred, dead-end filtration cell (Millipore) having an effective filtration area of 4.1 cm^2. Filtration cells were stirred at 500 rpm using a speed-adjustable stir plate (VWR) to prevent concentration polarization at the membrane surface. Transmembrane fluxes were measured by collecting each permeate in a container placed on top of a scale and observing the total weight increase over time. Permeation fluxes were calculated from the time derivatives of the accumulated weight.

The antifouling performance of the membranes was investigated directly from the time-dependent flux data for oil/water microemulsions containing 1000 ppm each of oleic acid (*cis*-9-octadecenoic acid, FW 282.47 g/mol) and triethanolamine (FW 149.19 g/mol) in dW. Nanoscale fractionation experiments were performed with cationic dyes rhodamine B (380 g/mol) and alcian blue (1299 g/mol), anionic dyes congo red (697 g/mol) and brilliant blue (854 g/mol), and vitamins B_2 (riboflavin, 376 g/mol) and B_{12} (cyanocobalamin, 1355 g/mol). The concentration of oleic acid or chromophore in the membrane permeate was determined by UV/vis spectroscopy using a Cary 5E spectrophotometer (Varian) over a wavelength range from 300 to 800 nm. Absorption spectra were calibrated using a series of standard solutions of known concentration.

III. Results and Discussion

PVDF-*g*-POEM Copolymer Morphology. Graft copolymer phase separation has been used previously to provide preferential transport across pervaporation and gas separation membranes, where the partial pressure of liquid or gas permeate species governs the permselectivity.[23,24] A significant advantage of this molecular architecture is its propensity to generate bicontinuous morphologies upon the local phase separation of backbone and side chains.[17,25−27] Here, PVDF-*g*-POEM copolymers incorporating grafted $POEM_9$ (∼8.5 ethylene oxide units, $T_g \sim -59.4$ °C) or $POEM_{23}$ (∼22.7 ethylene oxide units, $T_m \sim 36.2$ °C, $T_g \sim -58.3$ °C) macromonomers were synthesized, having number-average molecular weights (M_n) of 151 and 177 kg/mol, respectively, corresponding to POEM contents of 29 and 40 wt %.

The low compatibility between PVDF and poly(ethylene oxide), PEO, drives the microphase separation of backbone and side chains, even for short PEO chain lengths.[17,21] Figure 1 displays a TEM image of PVDF-

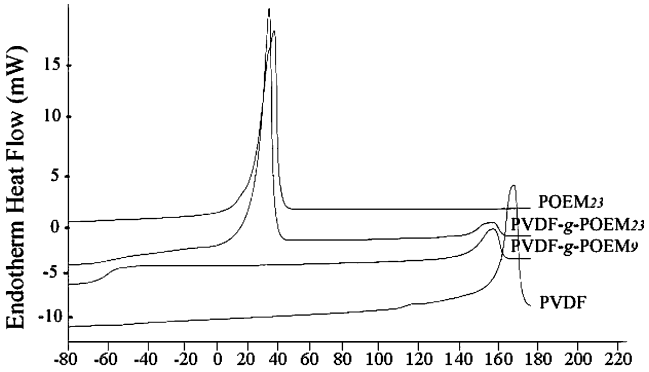

Figure 2. DSC thermograms for $POEM_{23}$ macromonomer, PVDF-*g*-$POEM_{23}$, PVDF-*g*-$POEM_9$, and parent PVDF.

g-$POEM_9$, in which POEM domains ~2 nm wide (dark regions) are observed. The resulting morphology gains structural integrity in water from the semicrystalline PVDF nanodomains (light phase). DSC data are consistent with a microphase-separated morphology, showing thermal signatures for both PVDF and POEM domains (Figure 2). DSC thermograms exhibit an endothermic peak due to the melting of PVDF crystallites at ~158 °C for both copolymers upon heating, compared with 169 °C for the parent PVDF. From the melting endotherms, the calculated percent crystallinity is reduced from 54% in the parent PVDF[22] to 15 and 6% in PVDF-*g*-$POEM_9$ and PVDF-*g*-$POEM_{23}$, respectively. X-ray diffraction patterns from both materials gave reflections consistent with the (110) and (220) planes of the monoclinic PVDF crystal structure. In addition, DSC traces for PVDF-*g*-$POEM_{23}$ show a second endothermic peak from the melting of poly(ethylene oxide) (PEO) side chains at ~33 °C.

PVDF offers limited solubility in aprotic solvents such as 1-methyl-2-pyrrolidinone (NMP), dimethylformamide (DMF), dimethylacetamide (DMAc), and dimethyl sulfoxide (DMSO) to allow solution-based film casting for subsequent membrane fabrication. POEM, by contrast, is compatible with a wide range of solvent media, except strongly nonpolar solvents such as hexane or petroleum ether. By keeping the POEM content below 60 wt %, the graft copolymers could be processed with PVDF-compatible solvents to create a stable selective layer that permits transport of a wide variety of liquids, including water, without dissolving.

Membrane Performance. The SEM image in Figure 3 reveals the cross-sectional morphology of a composite membrane comprising a ~3.5 μm layer of PVDF-*g*-$POEM_9$ coated onto a porous PVDF ultrafiltration membrane substrate. The surface of the copolymer film was smooth and nonporous to instrumental resolution. Contact angle measurements of a 1 μL water droplet on the composite membrane surface (Figure 4, right) exhibited instantaneous wetting as the water droplet spontaneously spread onto the surface. A continuous decrease in contact angle occurred until the droplet disappeared after 10 min, indicating water absorption into the POEM nanochannels of the self-assembled structure. By contrast, a PVDF control film (Figure 4, left) displayed hydrophobic behavior with a constant contact angle of 94.7 ± 0.4° over the duration of the experiment.

Pure water filtration studies confirmed the water permeability of the graft copolymer nanodomain structure. At 600 psi, the pure water flux from a ~500 μm

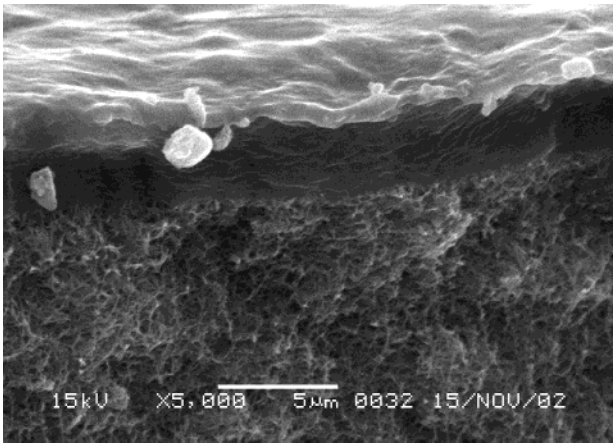

Figure 3. SEM cross-sectional image of composite membrane comprising a PVDF-*g*-$POEM_9$ film coated onto a porous PVDF membrane substrate. Scale bar is 5 μm.

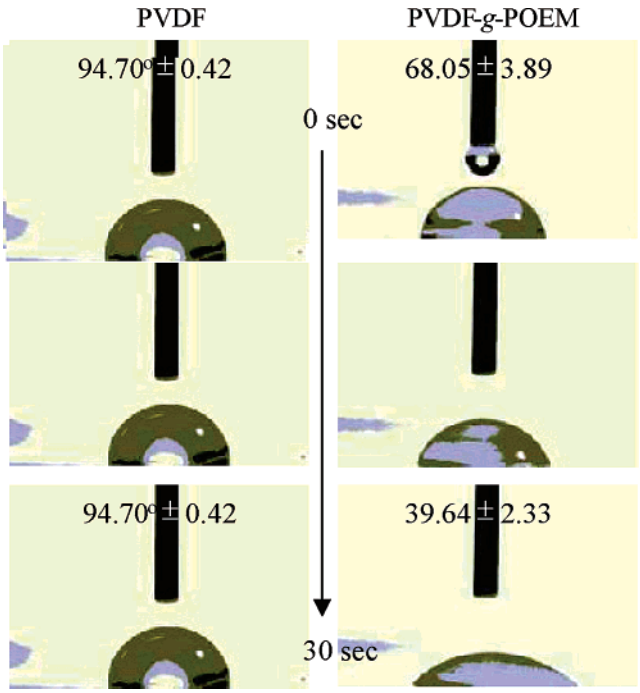

Figure 4. Contact angle measurements on PVDF-*g*-$POEM_9$-coated composite membrane (right) and PVDF film control (left).

free-standing PVDF-*g*-$POEM_9$ film was 17.25×10^{-4} gallons per square foot per day per psi (gfd/psi). Filtration through a composite membrane with a PVDF-*g*-$POEM_9$ coating ~3.5 μm thick such as that shown in Figure 3 resulted in water permeabilities of practical use (operating pressures below 100 psi), recording a pure water flux to 0.363 gfd/psi, at a transmembrane pressure of 66 psi. This value is somewhat above, but on the same order of magnitude as, pure water flux values of typical commercial NF membranes.[28] For example, a distilled water flux of 0.18 gfd/psi was reported for an Osmonics DS-5 DK membrane,[29] used as a control in the present study.

The utility of PVDF-*g*-POEM-coated membranes for filtration of oily feed solutions was demonstrated with the filtration of a model oil/water microemulsion containing 1000 ppm each of oleic acid (a fatty acid) and triethanolamine in deionized water (dW). Figure 5 plots the normalized flux (flux/initial flux) as a function of time for a PVDF-*g*-$POEM_9$-coated PVDF membrane and

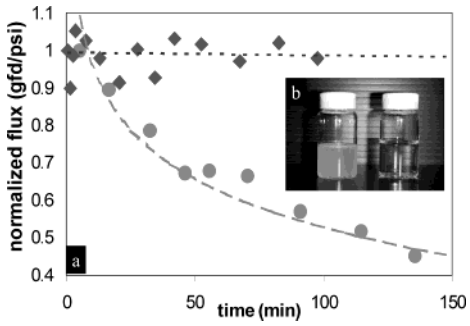

Figure 5. (a) Flux data from PVDF-*g*-POEM$_9$-coated membrane (◆) and Osmonics DS-5 DK NF membrane (●), normalized to the initial flux values of 0.275 and 0.027 gfd/psi, respectively. (b) Feed solution of oleic acid/triethanolamine/water microemulsion (left); permeate from filtration through a PVDF-*g*-POEM$_9$-coated composite membrane (right).

an Osmonics DS-5 DK thin film composite (polysulfone−polyamide) NF membrane[29] for oil/water separation applications. A steady flux is observed for the PVDF-*g*-POEM-coated membrane over the course of the 90 min filtration, with no detectable fouling. In contrast, the DS-5 membrane displays the typical exponential flux decline due to fouling when exposed to the same feed solution.[4] The initial flux for the PVDF-*g*-POEM$_9$ composite membrane was 0.275 gfd/psi, roughly 10 times that recorded for the DS-5 membrane (0.027 gfd/psi). After 90 min filtration, the PVDF-*g*-POEM membrane recorded a flux ~16 times that of the DS-5. The excellent fouling resistance of the PVDF-*g*-POEM$_9$ composite membrane may be attributed to the strong hydrogen-bonding ability of the PEO side chains, which act as a grafted brush layer at the membrane surface and within the water-filled nanochannels. The ether oxygen groups of POEM coordinate strongly with water molecules, precluding the adsorption of oleic acid to the membrane surface.[18]

From UV/vis spectroscopy of the permeate solution, the PVDF-*g*-POEM$_9$-coated membrane was found to display excellent retention of oleic acid (>99.9%, the resolution of the instrument). Note that the UV/vis method employed here is insensitive to the presence of TEA molecules dissolved in the permeate solution. Individual molecules of TEA might be expected to pass through the membrane nanochannels due to their small size (FW 149.19 g/mol) and compatible chemistry. Dissolved molecules with molecular cross sections larger than the effective nanochannel diameter, however, should be excluded from entering the membrane, allowing for size-based molecular fractionation. The effective width of the nanochannels is expected to be smaller than the POEM domains seen in Figure 1 and will depend on the degree of swelling of the PEO brush layer lining the channels.

The molecular sieving capability of the PVDF-*g*-POEM$_9$-coated membranes was investigated using like-

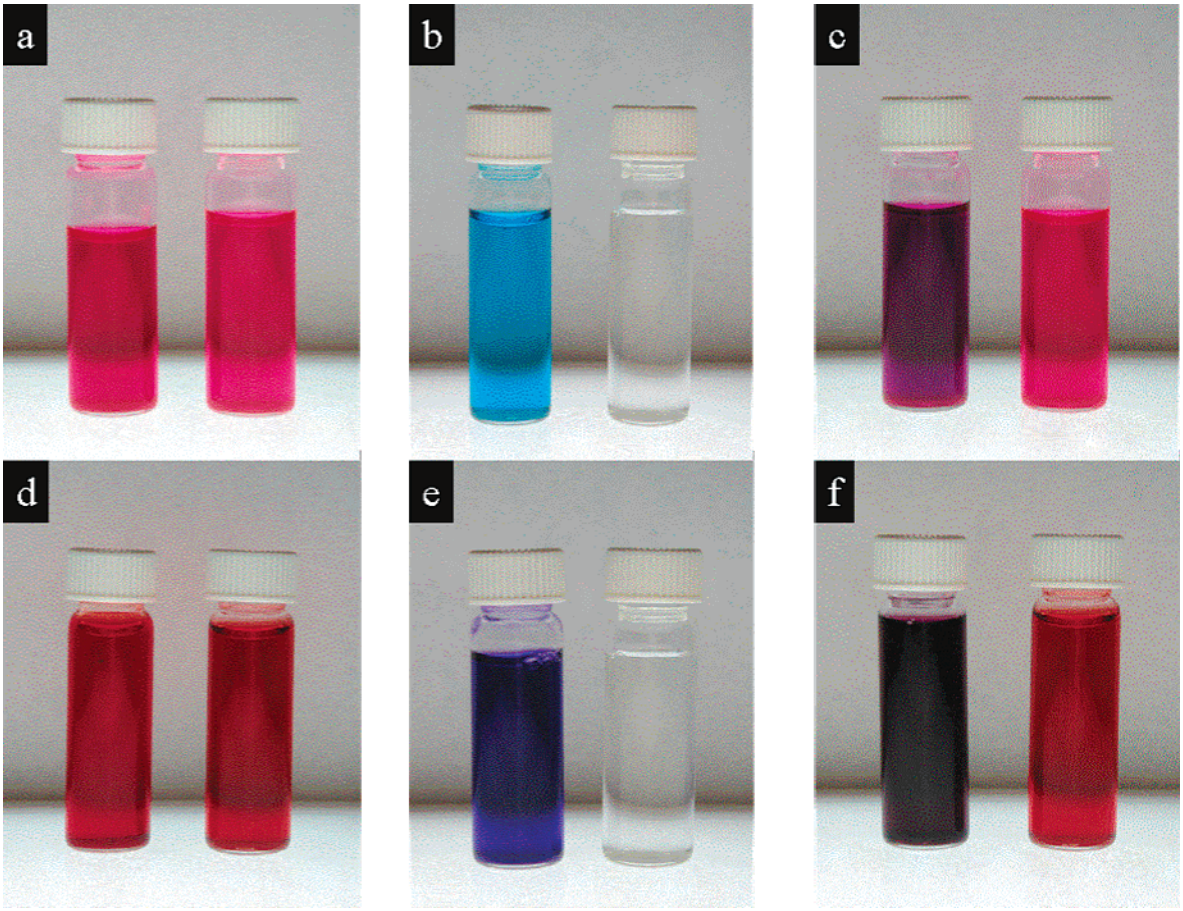

Figure 6. Top series: Filtration of 100 ppm positively charged dyes with PVDF-*g*-POEM$_9$-coated composite membranes: (a) Feed solution of rhodamine B in water (left) and permeate (right). (b) Feed solution of alcian blue in water (left) and permeate (right). (c) Feed solution of rhodamine B and alcian blue mixture in water (left) and permeate (right). Bottom series: Filtration of 100 ppm negatively charged dyes with PVDF-*g*-POEM$_9$ coated composite membranes. (d) Feed solution of congo red in water (left) and permeate (right). (e) Feed solution of brilliant blue in water (left) and permeate (right). (f) Feed solution of congo red and brilliant blue mixture in water (left) and permeate (right).

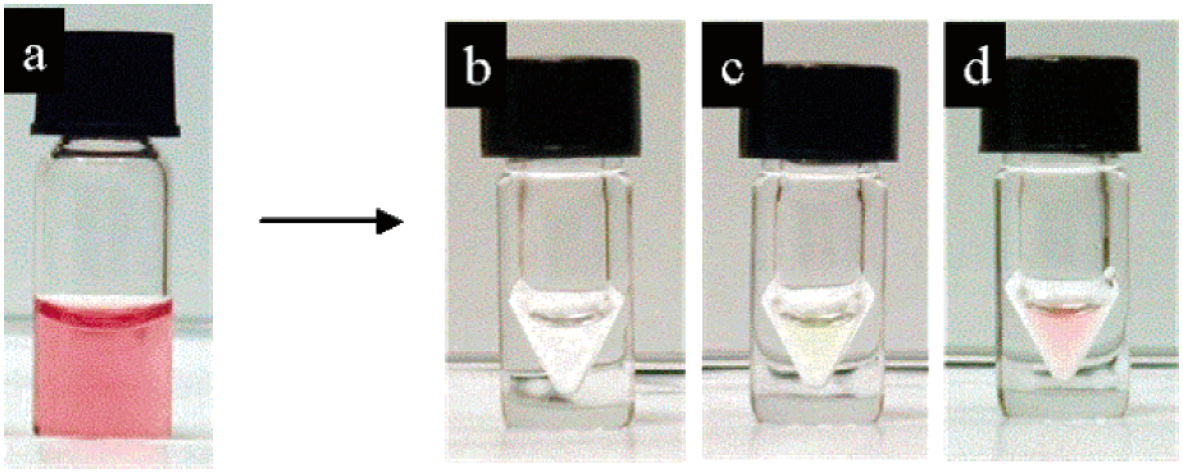

Figure 7. Time-dependent permeation of vitamin B mixture in aqueous solution through a ~500 μm PVDF-*g*-POEM$_{23}$ film: (a) Feed solution containing vitamin B_2 and B_{12} mixture in water. (b) Permeate at first hour containing only water. (c) Permeate at 12th hour containing vitamin B_2 and water. (d) Permeate at 24th hour containing vitamins B_2 and B_{12} and water.

charged molecular organic dyes dissolved in dW at 100 ppm. For feed solutions of two positively charged dyes, the composite membrane offered no retention (<0.1%, the instrument resolution) of the smaller rhodamine B dye (380 Da) of dimensions 15.1 × 11.9 × 5.9 Å^3 (Figure 6a) but complete retention (>99.9%) of the larger alcian blue dye (1299 Da) of dimensions 17.5 × 13.1 × 3.8 Å^3 (Figure 6b). These dyes vary in their limiting dimension by only a few angstroms, suggesting subnanometer selectivity. Such exclusion capability was reconfirmed by filtration of a feed solution containing a mixture of both dyes, where only rhodamine B dye was observed in the permeate solution (Figure 6c).

Alcian blue is known to form ionic aggregates through planar stacking that might affect its penetration into the POEM nanochannels. Hence, a second experiment was performed using two negatively charged dyes shown in Figure 6d−f, dissolved in dW at 100 ppm. The composite membrane displayed no retention (<0.1%) of congo red dye (697 Da), having dimensions 24.5 × 7.5 × 2.2 Å^3 (Figure 6d) but complete retention (>99.9%) of brilliant blue dye (854 Da), with dimensions 21.9 × 15.3 × 4.7 Å^3 (Figure 6e). Although congo red is a longer molecule than brilliant blue, it has a substantially smaller cross-sectional area. Hence, the congo red passes unobstructed through the POEM domains while brilliant blue is rejected. Filtration of dye mixtures yielded only congo red dye in the permeate (Figure 6f). As a control, the PVDF membrane substrate was tested using the same dye solutions and shown to exhibit no retention capability for these dyes.

We additionally examined whether PVDF-*g*-POEM membranes could function as a size-based chromatograph, separating molecules kinetically on the basis of molecular volume. Because molecular mobility scales inversely with molecular weight, the design of selective layers with longer diffusion pathways should render sufficient differences in elution time among permeates of different sizes to allow their separation. Such capability was demonstrated in the extraction of the smaller vitamin B_2 (riboflavin, 376 Da) of dimensions 12.1 × 10.3 × 3.8 Å^3 from vitamin B_{12} (cyanocobalamin, 1355 Da) of dimensions 22.1 × 11.3 × 5.8 Å^3 in the filtration of an aqueous mixture containing 100 ppm of each vitamin through a ~500 μm PVDF-*g*-POEM$_{23}$ film at 70 psi. As illustrated in Figure 7, after the first hour, the permeate contained only pure water, whereas at the 12th hour, both vitamin B_2 and water were detected, as confirmed by UV/vis. At the 24th hour, all species in the feed solution (vitamin B_2, vitamin B_{12}, and water) were observed in the permeate.

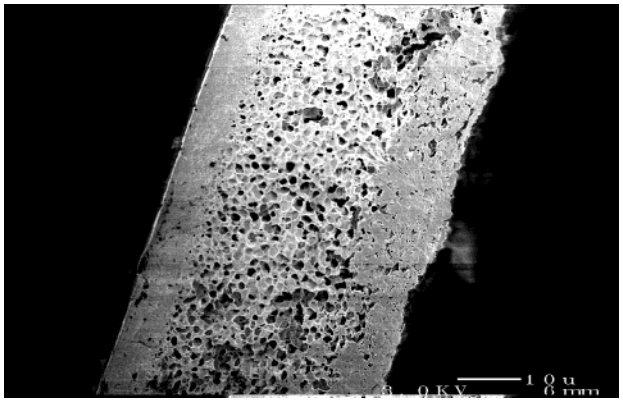

Figure 8. SEM cross-sectional image of PVDF-*g*-POEM$_9$/PVDF blend asymmetric membrane prepared by one-step immersion precipitation. PVDF-*g*-POEM$_9$ segregates to form a nonporous separating layer at the membrane top surface (left side of image). Scale bar is 10 μm.

The kinetically based separation of vitamins B_2 and B_{12} using the PVDF-*g*-POEM$_{23}$ thick film membrane can be explained by the flux dependence on the size of the diffusing species. With increasing Stokes radius or molecular volume, the diffusivity decreases, enabling B_2 to migrate through the film before B_{12}. The actual diffusion mechanism might be quite complex, however, encompassing features of classical solution-diffusion[30] as well as single-file diffusion[31,32] characteristic of nanochannel transport. Further work is planned to assess more quantitatively the transport mechanism in these films.

Finally, to create a molecular sieving membrane using a simple one-step fabrication process, a polymer solution incorporating a 75:25 (w:w) mixture of PVDF:PVDF-*g*-POEM$_9$ in DMAc was prepared and cast into an asymmetric membrane by immersion precipitation in deionized water. In keeping with the results of Hester et al.,[17,33−35] the amphiphilic graft copolymer segregates selectively to the membrane surface, creating in this instance a nonporous PVDF-*g*-POEM$_9$-rich separating layer, as shown in cross section in Figure 8. The separation characteristics and antifouling properties of

these one-step-fabricated membranes were found to be equivalent to that of thin film composites, with >99.9% oleic acid retention without fouling for the 1000 ppm model oil/water emulsion, complete retention (> 99.9%) of alcian blue and brilliant blue dyes in dW, and no retention (<0.1%) of rhodamine B and congo red dyes in dW. However, the pure water flux through this membrane ($\sim 4.43 \times 10^{-3}$ gfd/psi) fell substantially below that of the thin film composite membranes. Tuning the casting conditions should allow optimization of the membrane morphology to achieve commercially useful fluxes while retaining the observed antifouling character and subnanometer selectivity.

IV. Conclusions

Antifouling polymer membranes with subnanometer size-based separation capability were developed on the basis of molecular self-assembly of an amphiphilic PVDF-*g*-POEM copolymer. Their simplicity in fabrication renders these systems practical candidates for water recovery from oily waste streams as well as rapid throughput molecular-scale separations for applications in the chemical, biochemical, and pharmaceutical industries. The compatibility of PEO chemistry with most common organic solvents such as acetone, chloroform, toluene, tetrahydrofuran, ethanol, and methanol, combined with the lack of solubility of PVDF in most organic solvents, should offer great versatility for liquid-based separations.[28]

Acknowledgment. The authors acknowledge William McDonald and Jane Park for their assistance with membrane casting and characterization, Dr. Jian Qui and Dr. Sai Prakash at Pall Corp. for helpful discussions in the development of the thin film composite membranes, Simon C. Mui for his assistance with XRD, and Dr. You-Yeon Won for the TEM image. Financial support for this work was provided by the U.S. Office of Naval Research under Award N00014-02-1-0343. This work made use of MRSEC Shared Experimental Facilities supported by the National Science Foundation under Award DMR-0213282.

References and Notes

(1) Van der Bruggen, B.; Vandecasteele, C.; Van Gestal, T.; Doyen, W.; Leysen, R. *Environ. Prog.* **2003**, *22*, 46−56.
(2) Xu, Z. L.; Chung, T. S.; Huang, Y. *J. Appl. Polym. Sci.* **1999**, *74*, 2220−2233.
(3) Petersen, R. J. *J. Membr. Sci.* **1993**, *83*, 81−150.
(4) Faibish, R. S.; Cohen, Y. *Colloids Surf. A* **2001**, *191*, 27−40.
(5) Pontie, M.; Diawara, C.; Rumeau, M.; Aureau, D.; Hemmery, P. *Desalination* **2003**, *158*, 277−280.
(6) Awadalla, F. T.; Kumar, A. *Sep. Sci. Technol.* **1994**, *29*, 1231−1249.
(7) Christy, C.; Vermant, S. *Desalination* **2002**, *147*, 1−4.
(8) Burnouf, T.; Radosevich, M. *Haemophilia* **2003**, *9*, 24−37.
(9) Mulder, M. *Basic Principles of Membrane Technology*; Klewer Academic Publishers: Dordrecht, 1996.
(10) Jirage, K. B.; Hulteen, J. C.; Martin, C. R. *Science* **1997**, *278*, 655−658.
(11) Yu, S.; Lee, S. B.; Kang, M.; Martin, C. R. *Nano Lett.* **2001**, *1*, 495−498.
(12) Czaplewski, K. F.; Hupp, J. T.; Snurr, R. Q. *Adv. Mater.* **2001**, *13*, 1895−1897.
(13) Williams, M. E.; Benkstein, K. D.; Abel, C.; Dinolfo; P. H.; Hupp, J. T. *Proc. Natl. Acad. Sci. U.S.A.* **2002**, *99*, 5171−5177.
(14) Akthakul, A.; McDonald, W. F.; Mayes, A. M. *J. Membr. Sci.* **2002**, *208*, 147−155.
(15) Fleischer, R.; Price, P. *Science* **1963**, *140*, 1221−1222.
(16) Kesting, R. E. *Synthetic Polymeric Membranes*, 1st ed.; McGraw-Hill Book Co.: New York, 1971.
(17) Hester, J. F.; Banerjee, P.; Won, Y. Y.; Akthakul, A.; Acar, M. H.; Mayes, A. M. *Macromolecules* **2002**, *35*, 7652−7661.
(18) Harris, J. M. *Poly(ethylene glycol) Chemistry: Biotechnical and Biomedical Applications*; Plenum: New York, 1992.
(19) Beers, K. L.; Gaynor, S. G.; Matyjaszewski, K. *Macromolecules* **1998**, *31*, 9413−9415.
(20) Paik, H.-J.; Gaynor, S. G.; Matyjaszewski, K. *Macromol. Rapid Commun.* **1998**, *19*, 47−52.
(21) Inceoglu, S.; Olugebefola, S. C.; Acar, M. H.; Mayes, A. M. *Des. Monomers Polym.* **2004**, *7*, 181−189.
(22) Brandrup, J.; Immergut, E. H.; Grulke, E. A. *Polymer Handbook*; John Wiley & Sons: New York, 1999.
(23) Miyata, T.; Yamada, H.; Uragami, T. *Macromolecules* **2001**, *34*, 8026−8033.
(24) Uragami, T.; Yamada, H.; Miyata, T. *J. Membr. Sci.* **2001**, *187*, 255−269.
(25) Pochan, D. J.; Gido, S. P.; Pispas, S.; Mays, J. W. *Macromolecules* **1996**, *19*, 5099−5105.
(26) Pochan, D. J.; Gido, S. P.; Pispas, S.; Mays, J. W.; Ryan, A. Y.; Fairclough, J. P. A.; Hamley, I. W.; Terrill, N. J. *Macromolecules* **1996**, *29*, 5091−5098.
(27) Shinozaki, A.; Jasnow, D.; Balazs, A. C. *Macromolecules* **1994**, *27*, 2496−2502.
(28) Bhuanashali, D.; Bhattacharyya, D. *Ann. N.Y. Acad. Sci.* **2003**, *984*, 159−177.
(29) Koyuncu, I. *J. Chem. Technol. Biotechnol.* **2003**, *78*, 1219−1224.
(30) Wijmans, J. G.; Baker, R. W. *J. Membr. Sci.* **1995**, *107*, 1−21.
(31) Keffer, D. *Chem. Eng. J.* **1999**, *74*, 33−42.
(32) Wei, Q.-H.; Bechinger, C.; Leiderer, P. *Science* **2000**, *287*, 625−627.
(33) Hester, J. F.; Banerjee, P.; Mayes, A. M. *Macromolecules* **1999**, *32*, 1643−1650.
(34) Hester, J. F.; Olugebefola, S. C.; Mayes, A. M. *J. Membr. Sci.* **2002**, *208*, 375−388.
(35) Hester, J. F.; Mayes, A. M. *J. Membr. Sci.* **2002**, *202*, 119−135.

MA048837S